Cancer Management and Research

Dovepress
open access to scientific and medical research

Open Access Full Text Article

ORIGINAL RESEARCH

RETRACTED ARTICLE: Downregulation of PIM1 regulates glycolysis and suppresses tumor progression in gallbladder cancer

This article was published in the following Dove Press journal:
Cancer Management and Research

Chen Xue[1,2,*]
Yuting He[1,2,*]
Qiuyue Hu[1,2]
Yan Yu[1,2]
Xiaolong Chen[1,2]
Jianan Chen[1,2]
Fang Ren[2]
Juan Li[1,2]
Zhigang Ren[1,2]
Guangying Cui[1,2]
Ranran Sun[1–3]

[1]Precision Medicine Center, The First Affiliated Hospital of Zhengzhou University, Zhengzhou 450052, China; [2]Key Laboratory of Clinical Medicine, The First Affiliated Hospital of Zhengzhou University, Zhengzhou 450052, China; [3]National Engineering Laboratory for Internet Medical Systems and Applications, The First Affiliated Hospital of Zhengzhou University, Zhengzhou 450052, China

*These authors contributed equally to this work

Background: PIM1, a serine/threonine kinase, plays an essential role in tumorigenesis of multiple types of tumors. However, the expression pattern and functions of PIM1 in gallbladder cancer (GBC) remain largely unknown.

Materials and methods: Immunohistochemistry, quantitative real-time PCR, and western blot analysis were performed to measure the expression of PIM1. Tissue microarray analysis was used to confirm the relationship between PIM1 expression and clinical outcomes of GBC patients. Finally, in vivo and in vitro functional studies were performed to detect the inhibition of PIM1 by RNAi or specific inhibitor in GBC cells.

Results: We observed that PIM1 was dramatically overexpressed in GBC tissues, and its expression levels were positively related with clinical malignancies and a poor prognosis. Inhibition of PIM1 via RNAi or enzyme-specific inhibitor could suppress GBC cell proliferation, migration, and invasion both in vitro and vivo. Additionally, flow cytometry assays and cell cycle assays indicated that PIM1 inhibition promoted cell apoptosis and induced cell cycle arrest. Remarkably, inhibition of PIM1 could drive a metabolic shift from aerobic glycolysis to oxidative phosphorylation. We found that inhibition of PIM1 mechanistically reduced glucose consumption by regulating key molecules in aerobic glycolysis.

Conclusion: PIM1 may serve as an oncogene in GBC and be involved in the regulation of glycolysis. PIM1 is a promising therapeutic target for the treatment of human GBC.

Keywords: PIM1, gallbladder cancer, aerobic glycolysis, tumor progression

Introduction

Gallbladder cancer (GBC) is the most common malignancy of biliary tract.[1] Recently, therapeutic options for advanced GBC are limited and surgical resection is the mainstay of therapy for GBC patients, which is not suitable for patients with advanced stage cancer.[2,3] The dismal clinical outcomes of advanced GBC are largely due to inevitable recurrence and metastasis after surgery.[4] However, the underlying molecular mechanisms of GBC progression remain unclear.[5] It is thus critical to identify novel biomarkers for early detection and creation of effective therapeutic strategy for GBC patients.

PIM1 belongs to the family of serine/threonine kinases. Increasing evidence has shown that upregulated PIM1 plays a crucial part in tumor progression in a variety of tumors,[6] including breast cancer,[7] glioblastoma multiforme,[8] bladder cancer,[9] and hepatocellular carcinoma,[10] highlighting its role as a potential oncogene. Nevertheless, the expression pattern and functional role of PIM1 in GBC are still unknown and require more investigation.

Correspondence: Ranran Sun
Precision Medicine Center, The First Affiliated Hospital of Zhengzhou University, No. 1 Jianshe East Road, Zhengzhou 450052, Henan, China
Tel +86 371 6796 6905
Email sunran1986318@163.com

submit your manuscript | www.dovepress.com
Dovepress
http://dx.doi.org/10.2147/CMAR.S184381

The Warburg effect, a unique metabolic phenotype of cancer, describes how cancer cells preferentially make use of glucose through aerobic glycolysis.[11,12] Aerobic glycolysis supports the rapid proliferation of cancer cells and thus tumor growth.[13,14] There is growing evidence that several essential glycolytic enzymes, such as LDHA,[15] PGK1,[16] GLUT1,[17] and PKM2,[18] could promote malignancy in GBC. Interestingly, one study has reported that upregulation of PIM1 could regulate glycolysis and promote tumor progression through the PI3K/AKT pathway in hepatocellular carcinoma,[10] indicating that PIM1 may promote tumor growth, at least in part, by regulating aerobic glycolysis.

In this study, we confirmed that PIM1 was upregulated and correlated with poor clinical outcomes in GBC patients. We then inhibited PIM1 via RNAi or enzyme-specific inhibitor to suppress GBC cell proliferation, migration, and invasion in vitro and tumor growth in vivo. Additionally, PIM1 inhibition caused the rate of cell apoptosis to increase and induce cell cycle arrest. Furthermore, downregulation of PIM1 could suppress glucose metabolism via regulating key molecules in aerobic glycolysis. Taken together, these findings demonstrate a novel mechanism for the regulation of aerobic glycolysis in GBC.

Materials and methods

Clinical tissues

Tissue microarray (TMA) was performed as described previously.[15] Briefly, 53 GBC samples and 37 pair tumorous gallbladder samples were used to construct our tissue microarray. Another TMA containing 79 GBC tissues and 20 non-tumorous specimens was purchased from Outdo Biotech (Shanghai, China). After approval by the ethical committee of the First Affiliated Hospital of Zhengzhou University, written informed consent was obtained from the patients, and this was conducted in accordance with the Declaration of Helsinki. Then clinical information was collected, including age, gender, TNM stage, distant metastasis, tumor size, histologic grade, as well as follow-up months (Tables 1 and 2).

Immunohistochemistry (IHC) analysis

IHC was performed as described previously.[15] In addition, we established a scoring system of PIM1 expression that divided PIM1 expression levels into five stratifications according to the different intensities of PIM1 staining. Simultaneously, scores 1+, 2+, and 3+ were defined as low expression, while scores 4+ and 5+ were deemed as high expression for statistical analysis.

Cell lines and cell culture

The human GBC cell lines in this study, GBC-SD, NOZ, OCGU-1, and SGC-996, were purchased from Academy of Sciences (Shanghai, China) and maintained in DMEM (Gibco, Waltham, MA, USA) medium with 10% fetal bovine serum (Gibco). They were incubated in a CO_2 incubator (5% CO_2/95% air) at 37°C. Relevant details are shown in Table S1.

Western blotting

Total protein was isolated from GBC cells using RIPA buffer and then protein concentration was examined. Second, 20 µg protein samples were loaded onto 12% SDS-PAGE (Invitrogen, Carlsbad, CA, USA) and then the samples were transferred from the gel to the nitrocellulose membranes (Millipore, Billerica, MA, USA). After being blocked with blocking buffer (Invitrogen), the membranes were incubated with primary antibody. They were then washed three times

Table 1 The relationship between PIM1 expression and clinicopathological features of gallbladder carcinoma

Clinicopathological features		No. of cases	PIM1 expression		*P*-value
			Low (n=33)	High (n=33)	
Age (years)	< Median	33	15	18	0.311
	> Median	33	18	15	
Gender	Male	19	11	8	0.294
	Female	47	22	25	
Tumor size	<4 cm	31	13	18	0.162
	>4 cm	35	20	15	
TNM stage	Stage I and II	31	20	11	0.026
	Stage III and IV	35	13	22	
Distant metastasis	Absent	37	24	13	0.006
	Present	29	9	20	
Histologic grade	Grade I and II	28	18	10	0.046
	Grade III and IV	38	15	23	

Table 2 Univariate and multivariate analyses of overall survival of gallbladder carcinoma

	Clinicopathological features	Univariate analyses			Multivariate analyses		
		HR	95% CI	*P*-value	HR	95% CI	*P*-value
Age (years)	< Median	1.000	0.607–1.998	0.750		0.659–2.837	0.490
	> Median	1.102					
Gender	Male	1.000	0.399–1.508	0.454		0.297–1.368	0.248
	Female	1.289					
Tumor size	<4 cm	1.000	0.664–2.168	0.547		0.513–1.824	0.917
	>4 cm	1.199					
TNM stage	Stage I–II	1.000	2.296–8.919	<0.001	1.000	1.574–7.430	0.002
	Stage III–IV	4.525			3.170		
Histologic grade	Stage I–II	1.000	1.616–5.666	0.001	1.000	0.891–3.385	0.105
	Stage III–IV	3.026			2.022		
Distant metastasis	Absent	1.000	1.448–5.783	0.003	1.000	.153–4.941	0.019
	Present	2.894			2.506		
PIM1 expression	Low	1.000	1.405–2.673	<0.001	1.000	93–2.319	0.015
	High	1.987			1.3		

Abbreviation: PIM1, provirus integration site for Moloney murine leukemia virus 1.

in PBST and membranes were then incubated with HRP-conjugated secondary antibody. In the end, the signal strength was determined via the chemiluminescent staining. The primary antibodies used in this study are shown in Table S2.

PIM1 inhibitor and siRNA/lentiviral transfection

PIM1 inhibitor, SGI-1776, was commercially purchased from Merck Millipore (Darmstadt, Germany). GBC-SD and NOZ cells were transfected with PIM1-shRNA (Shanghai, China) using Lipofectamine 3000 transfection reagent (Invitrogen), according to the manufacturer's instructions. Sequences of shRNA targeting PIM1 (sh-PIM1) were synthesized by Hanheng (Shanghai, China). The constructed lenti-sh-PIM1 or lenti-NC-shCK was transfected into GBC-SD cells, respectively, using Lipofectamine 3000 transfection reagent (Invitrogen). After being treated with puromycin for 4 weeks, we obtained the stable GBC-SD cell lines downregulating PIM1. The primer sequences used in this study are presented in Table S3.

Cell proliferation assay

A CCK-8 Kit was utilized to assess cell growth. Transfected and non-transfected human GBC-SD or NOZ cells were plated in the 96-well plate. At the established time point, they were inoculated with 100 µL 2-(2-methoxy-4-nitrophenyl)-3-(4-nitrophenyl)-5-(2, -4-disulfobenzene)-2H-tetrazolium monosodium salt (WST-8) (Beyotime, Jiangsu, China) and then incubated for 4 hours at 37°C. Plate absorbance at 570 nm was by a spectrophotometer (Molecular Devices LLC, Sunnyvale, CA, USA).

EDU kit (RiboBio, Guangzhou, China) was performed to detect cell proliferation viability. Images were obtained and analyzed with a microscope at 100× (Olympus, Tokyo, Japan). The ratio of EDU-stained cells (with red fluorescence) to DAPI-stained cells (with blue fluorescence) was calculated to evaluate the cell proliferation activity.

Colony formation assays were further applied to identify the effect of downregulated PIM1 on GBC cell growth. We diluted and plated the transfected cells in six-well plates at 2,000 cells per well. After 10 days of incubation, colonies were fixed, stained, and counted.

Cell migration and invasion assay

For cell migration analysis, wound-healing assay was performed. Cells were seeded in the six-well plates and subjected to different chemical treatments. When the cells reached about 90% confluency, a wound was scratched with a sterile plastic tip and then cultured for 48 hours. At the indicated time points, images were taken under a microscope.

Our cell invasion assay used Matrigel Invasion Chambers (BD Biosciences, San Jose, CA, USA). In brief, 1×10^4 transfected cells were cultured on the upper chamber of the Transwell insert in serum-free medium, with the bottom chamber filled with DMEM and 10% FBS. After 24 hours, invasive cells were stained with 0.5% crystal violet, then photographed and counted.

Cell cycle distribution analysis

GBC-SD cells were harvested and treated with 10 µmol/L SGI-1776 for 96 hours, and then they were fixed in 75% ice-cold ethanol overnight and resuspended in PI staining buffer

at 4°C for 30 minutes after washing twice with cold PBS. Cell cycle distributions among the samples were then examined using a flow cytometer (Calibur, Franklin Lake, NJ, USA).

Tumor xenograft model

The Animal Care Committee of the First Affiliated Hospital of Zhengzhou University approved all animal experiments in this study, and written confirmation that all experiments were performed following the First Affiliated Hospital of Zhengzhou University and national guidelines and regulations was obtained. We purchased BALB/c-nude mice from Beijing Vital River Laboratory Animal Technology (Beijing, China). Approximately 5.0×10^6 GBC-SD cells transfected with PIM1 shRNA (sh-PIM1) or MOCK-shRNA (MOCK) were injected subcutaneously into left flanks. The resulting tumor sizes were assessed and imaged every week, and tumor-carrying mice were euthanized in 6 weeks. The IVIS@ Lumina II imaging system, purchased from Caliper Life Sciences (Hopkinton, MA, USA), was used after an intraperitoneal injection of 4.0 mg of luciferin (Gold Biotechnology, Olivette, MO, USA) in 50 µL of saline. At completion, tumor specimens were weighed and fixed in 10% formalin and embedded in paraffin, and then stained with hematoxylin and eosin for analysis.

Glucose uptake, lactate, and ATP assays

A Glucose Uptake Colorimetric Assay Kit was used to measure glucose uptake. In total, 1×10^6 GBC cells with PIM1 inhibitor were seeded in a 6-well plate and then starved for glucose by pre-incubating with 100 µL Krebs-Ringer-Phosphate-HEPES buffer containing 2% BSA for 40 minutes. After incubation with 10 µL of 10 mmol/L 2-DG, glucose consumption was measured.

In addition, we employed a Lactate Assay Kit II and ATP Colorimetric Assay Kit to measure lactate and ATP production, respectively (Biovision, Milpitas, CA, USA). Here, 1×10^6 cells were homogenized in 100 µL corresponding assay buffer provided with the kits. Samples were centrifuged, and the soluble fraction was assayed.

Quantitative real-time PCR (qRT-PCR)

Trizol reagent (Invitrogen) was used to extract total RNA in GBC-SD cells according to the protocol as described previously.[19] Briefly, NanoDrop 8000 spectrophotometer (Thermo Fisher Scientific, Waltham, MA, USA) was used to detect the concentration of RNA. Additionally, total RNA was reverse transcribed with TransScript First-Strand cDNA Synthesis SuperMix (TransGen, Beijing, China). qRT-PCR was performed on 7500 sequence detection system. Data were analyzed using the comparative Ct method ($2^{-\Delta\Delta Ct}$). Each group included three repeated wells. The primer sequences used in the study were shown in Table S4.

Glycolysis stress test

The procedure for measurements of the extracellular acidification rates (ECARs) was performed as described previously.[19] Briefly, we assessed the effect of PIM1 inhibition on glycolysis stress using the Seahorse XF96 Glycolysis Analyzer (Seahorse Bioscience, North Billerica, MA, USA).

Statistical analysis

SPSS 23.0 and GraphPad Prism 7.0 were used for all statistical analyses. The correlation between PIM1 expression and survival was determined with Kaplan–Meier analysis. Independent prognostic factors were analyzed using univariate and multivariate Cox proportional hazard regression models. Results were expressed as mean ± SD, and $P<0.05$ was considered to represent statistical significance.

Results

PIM1 is upregulated and associated with a poor prognosis in GBC

In order to detect PIM1 expression in GBC tissues, IHC analysis was performed in TMA, and the results are shown in Figure 1A and B. We observed that PIM1 was significantly increased in GBC tissues compared with adjacent nontumorous tissues (Figure 1C and D). In addition, our results revealed that PIM1 was notably increased in GBC patients with distant metastases (Figure 1E) and late TNM staging (III–IV stages) (Figure 1F). Subsequently, Kaplan–Meier analysis showed that patients with elevated expression of PIM1 patients had a markedly poorer overall survival (OS) than those with lower expression patients (Figure 1G). A forest plot of pooled HR depicting correlations between the indicated clinical criteria and OS is shown in Figure 1H. Taken together, these results validated that PIM1 was significantly upregulated and associated with poor clinical outcomes in GBC.

High expression of PIM1 is an independent adverse prognostic factor

We next investigated the correlation between PIM1 expression and clinical features of GBC patients. The clinicopathological features of the GBC patients are summarized in Table 1. Upregulated PIM1 expression was positively correlated with TNM stage ($P=0.026$), distant metastasis

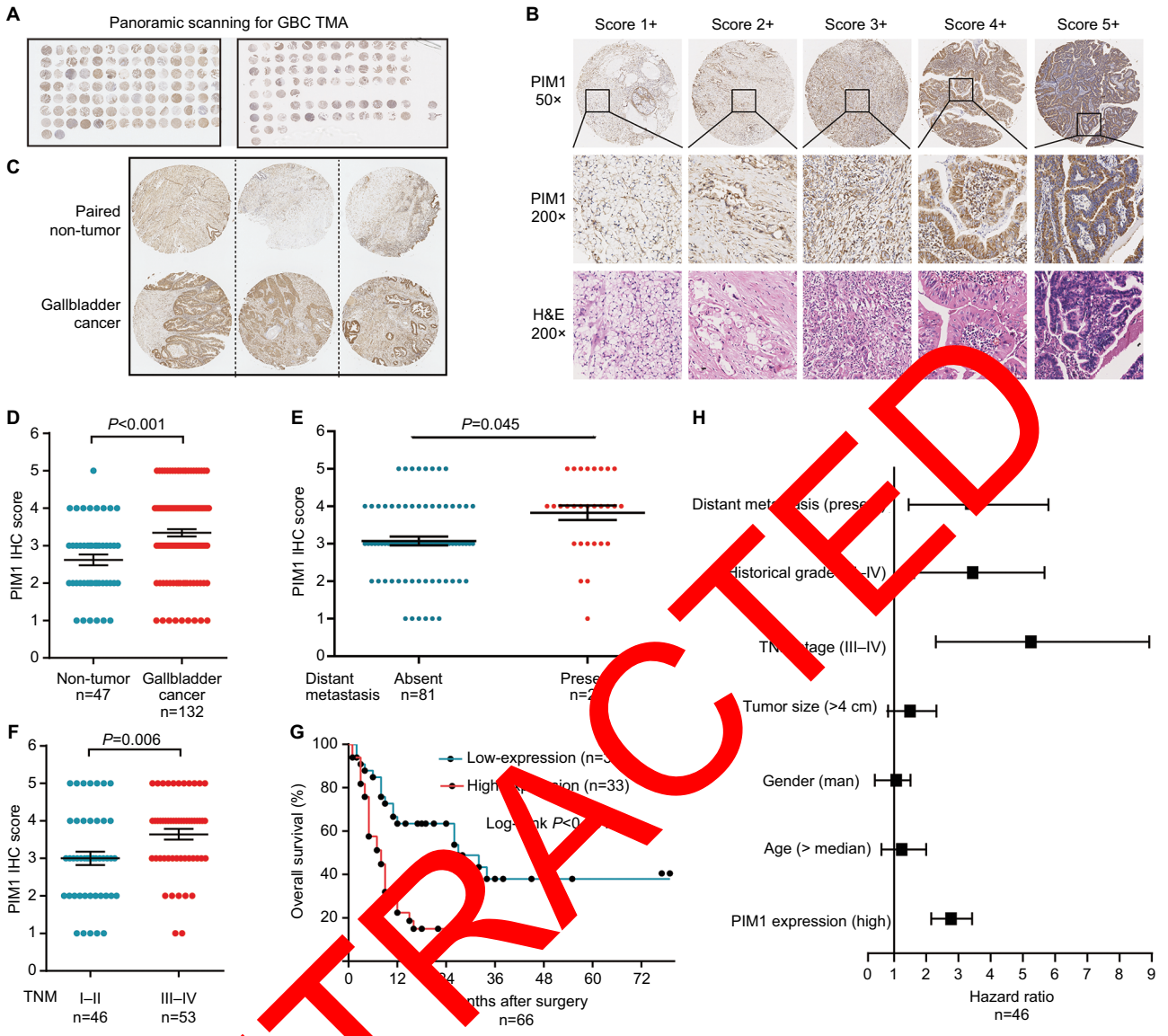

Figure 1 PIM1 is overexpressed in GBC tissues and negatively correlated with survival.

Notes: (**A**) Panoramic scanning for GBC TMA. Magnification ×1. (**B**) Representative PIM1 and immunohistochemical staining patterns with different staining scores in GBC tissues. (**C**) Representative PIM1 staining in GBC tissues and normal samples. Magnification ×50. (**D**) Histological scoring of PIM1 in GBC tissues and normal samples ($P<0.001$). (**E**) Distribution of PIM1 immunohistochemical staining scores in GBC tissues with or without metastasis ($P=0.045$). (**F**) Histological scoring of PIM1 according to TNM classification ($P=0.006$). (**G**) Kaplan–Meier survival analysis between expression of PIM1 (red, high PIM1 expression; green, low PIM1 expression) ($P<0.001$). (**H**) Univariable analysis using additional clinical information. Forest plot depicted correlations between the indicated clinical criteria and the overall survival of GBC patients.

Abbreviations: GBC, gallbladder cancer; TMA, tissues microarray.

($P=0.006$), and histologic grade ($P=0.049$). There was no significant correlation among the PIM1 expression and patient age, gender, and tumor size (Table 1).

Subsequently, univariable and multivariable Cox regression analyses were performed to clarify the risk factors correlated with GBC patients' prognosis. Univariable analyses demonstrated that TNM stage, histologic grade, distant metastasis, and PIM1 expression level were significant prognostic factors for prediction of OS in GBC. Meanwhile, multivariable analysis suggested that TNM staging (III and IV stages), distant metastasis, and PIM1 expression (high) were independent predictors for OS prediction (Table 2). Collectively, these data demonstrated that PIM1 may be a predictor for prognosis in GBC patients.

Knockdown of PIM1 decreases GBC cells proliferation, migration, and invasion ability

In order to further validate the role of PIM1 in GBC, functional experiments were performed in vitro. We found that

there was higher expression of PIM1 in NOZ and GBC-SD cells, but modest expression in OCGU-1 and SGC-996 (Figure 2A). Next, the efficiency of PIM1-siRNA was confirmed in NOZ and GBC-SD via western blot analysis. Our results showed that RNAi-mediated PIM1 silencing in GBC cells acted in a dose-dependent manner (Figure 2B). The suppressive effect of PIM1 downregulation on cell proliferation in GBC cells was confirmed by CCK-8 assay and EDU staining (Figure 2C and D). Furthermore, colony formation assay demonstrated that knockdown of PIM1 obviously suppressed the proliferation in GBC-SD and NOZ cells (Figure 2E). Moreover, wound-healing assay showed that downregulation of PIM1 markedly decreased the migration rate in both GBC-SD and NOZ cells (Figure 2F). Additionally, transwell invasion assays showed that the repression of PIM1 significantly reduced the invasion abilities of GBC-SD

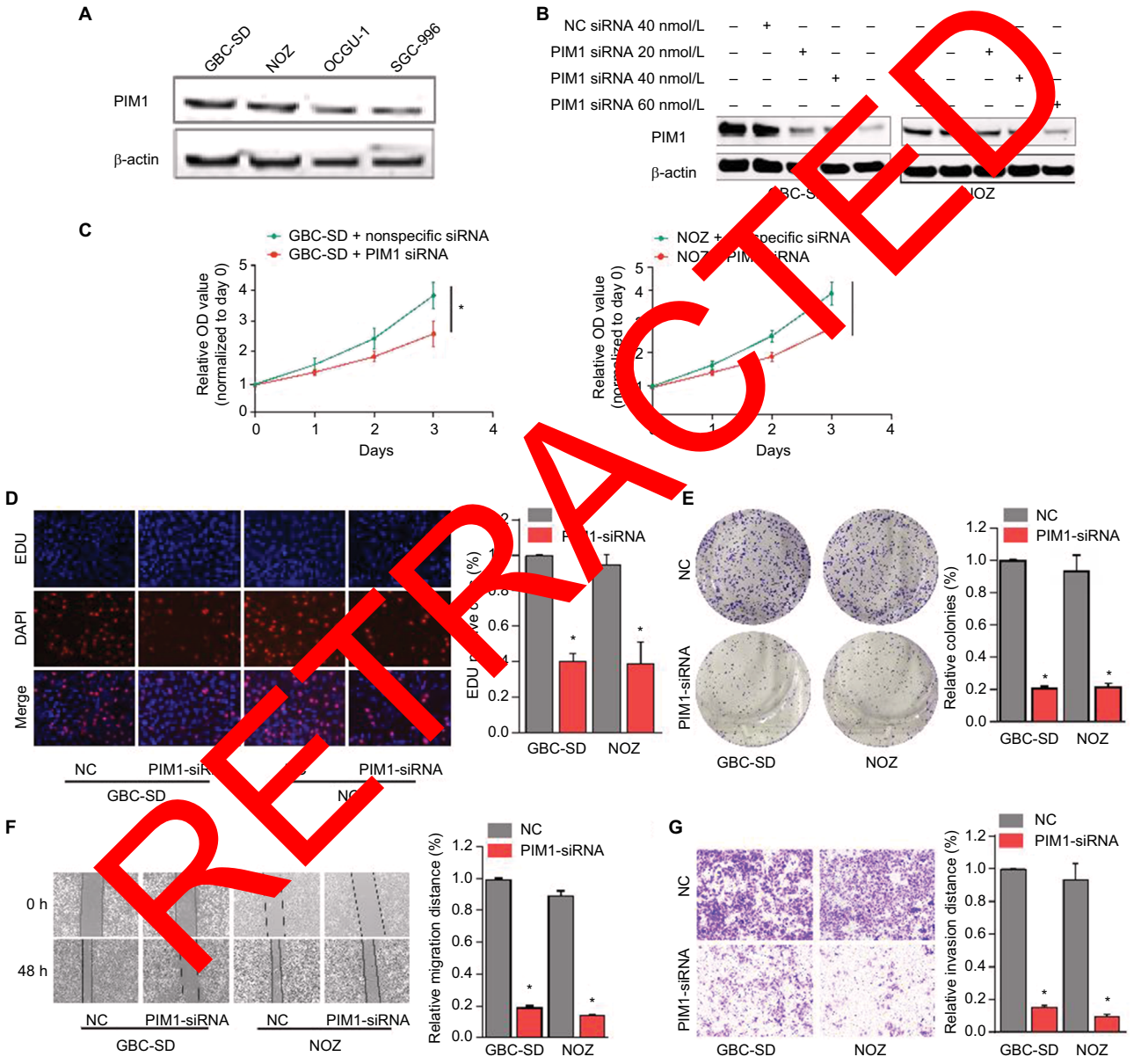

Figure 2 Expression of PIM1 in GBC cell lines and RNAi-mediated PIM1 silencing suppresses in vitro GBC cell proliferation, migration, and invasion.

Notes: (**A**) Expression levels of PIM1 in GBC cell lines were determined by western blotting. Expression of PIM1 was higher in GBC-SD and NOZ, compared to the expression in OCUG1 and SGC-996. (**B**) Dose-dependent PIM1 siRNA downregulated the expression of PIM1. (**C**) CCK-8 assay showed that PIM1 silencing attenuated proliferation of GBC-SD and NOZ cells. (**D**) EDU assay confirmed that PIM1 silencing suppress proliferation of GBC-SD and NOZ cells. Scale bar=50μm. (**E**) The colony formation ability of GBC-SD and NOZ cells was decreased when treated with PIM1 siRNA. Scale bar=5mm. (**F**) PIM1 silencing caused a remarkable suppression of cell migration in GBC-SD and NOZ cells using wound-healing assay. (**G**) The invasiveness of GBC-SD and NOZ cells infected with PIM1-siRNA was significantly suppressed according to cell invasion assay.

Note: *$P<0.05$.

Abbreviations: GBC, gallbladder cancer; NC, nonspecific control siRNA.

and NOZ cells (Figure 2G). These results collectively suggested that knockdown of PIM1 suppressed cell proliferation, migration, and invasion in vitro.

SGI-1776 inhibits proliferation and promotes apoptosis in GBC cells

To further confirm the effect of PIM1 downregulation on GBC cells, SGI-1776, a special inhibitor of PIM1, was adopted to treat GBC cells. As shown in Figure 3A, PIM1 expression obviously decreased in SGI-1776-treated group compared with the control group. Meanwhile, cell proliferation was dramatically inhibited after treatment with SGI-1776 by CCK-8 assay and EDU staining (Figure 3B and C). Moreover, our colony formation assay demonstrated the compromised colony-forming ability of SGI-1776-treated cells (Figure 3D).

We also examined the effects of SGI-1776 on the apoptosis of GBC cells. Flow cytometer analysis showed that apoptosis rates were significantly increased in SGI-1776-treated GBC-SD cells (Figure 3E). Additionally, cell cycle analysis showed that SGI-1776 could arrest the cell cycle at phase G0/G1 in GBC-SD cells (Figure 3F). Collectively, these results further confirmed that inhibition of PIM1 via inhibition with SGI-1776 could suppress cell proliferation, promote apoptosis, and induce cell cycle arrest in GBC cells.

Downregulation of PIM1 suppresses glycolysis of GBC cell

Based on this observation, we hypothesized that PIM-1 might regulate glycolysis in GBC cells.

As expected, inhibition of PIM treated with SGI-1776 caused a dramatic decrease in glucose consumption

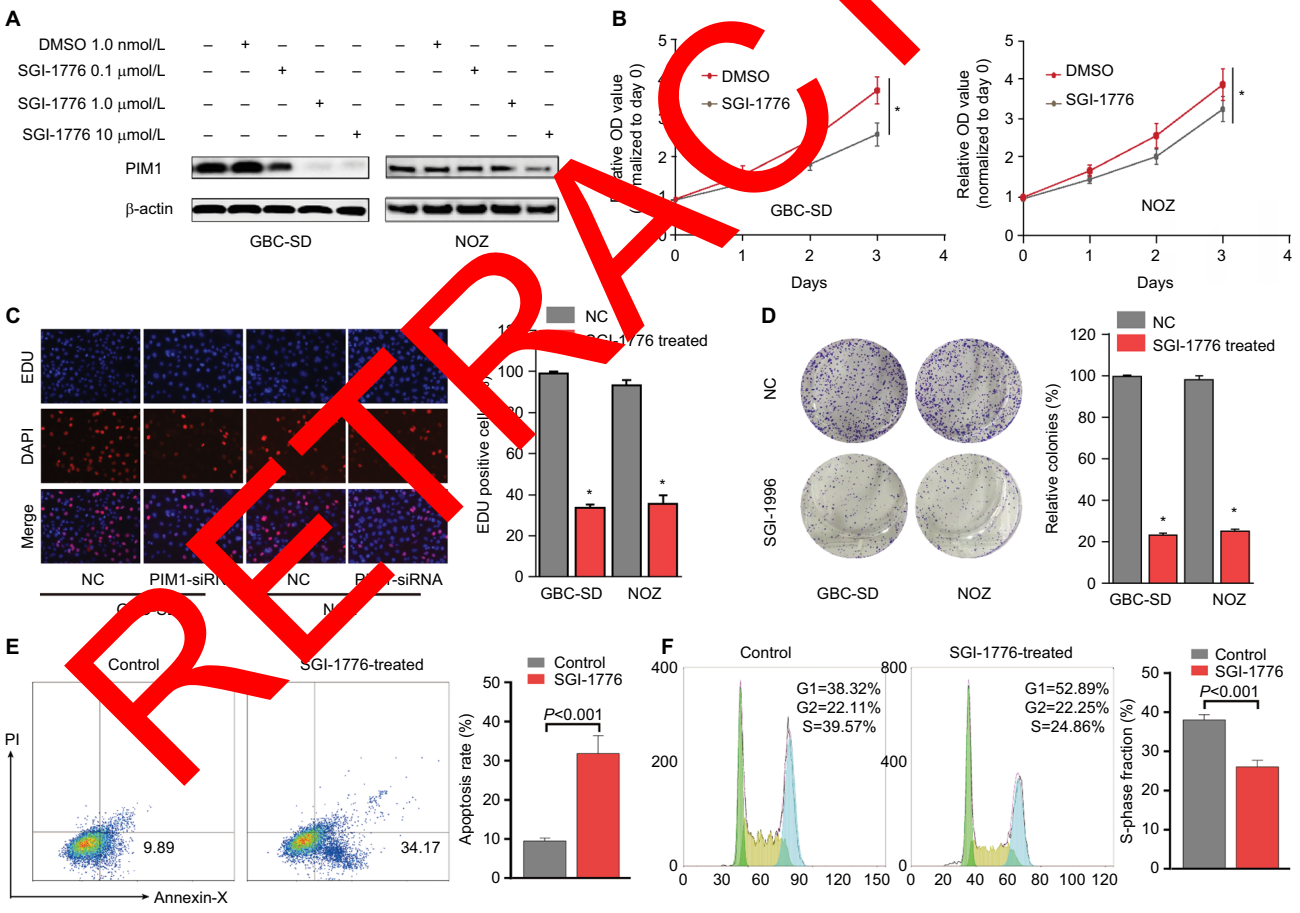

Figure 3 Downregulation of PIM1 by SGI-1776 inhibits proliferation, colony formation, and cell cycle of GBC cells in vitro.

Notes: (**A**) Treatment with SGI-1776 inhibited the expression of PIM1 in a dose-dependent manner in GBC cells. (**B**) CCK-8 assay showed that incubation with SGI-1776 suppressed proliferation of GBC-SD and NOZ cells. (**C**) EDU assay showed that treatment with PIM1 inhibitor SGI-1776 could suppress proliferation of GBC-SD and NOZ cells. Scale bar=50μm. (**D**) The colony formation ability of GBC-SD and NOZ cells was decreased when treated with SGI-1776. Scale bar=5mm. (**E**) The apoptosis in the early stage was significantly induced with SGI-1776 treated in GBC-SD cells through flow cytometer analysis. (**F**) SGI-1776 could arrest the cell cycle at phase G0/G1 in GBC-SD cells.

Note: *P<0.05.

Abbreviations: GBC, gallbladder cancer; NC, nonspecific control siRNA.

(Figure 4A) and cellular ATP level in GBC cells (Figure 4B), as well as lower lactate production compared to the negative control group (Figure 4C). In addition, we detected essential glycolytic enzymes involved in the Warburg effect, and found the protein and mRNA expression of PKM2, LDHA, and PGK1 were signally decreased in PIM1-inhibied group (Figure 4D and E). These results indicated that PIM1 may regulate glycolysis via regulation of essential glycolytic enzymes involved in the Warburg effect. In addition, to further clarify whether PIM1 promotes glucose metabolism in GBC cells, we performed the Seahorse assay to analyze the glycolytic flux based on ECAR. Basal glycolysis was significantly inhibited, whereas the maximal glycolytic capacity was notably decreased (Figure 4F–I). Impressively, these data collectively suggested that PIM1 contributes greatly to the metabolic shift between oxidative phosphorylation and glycolysis in GBC cells.

Inhibition of PIM1 inhibits GBC tumor genesis in vivo

Subsequently, we developed a nude mouse xenograft model to further verify the effect of PIM1 silencing on tumor growth in vivo. A dynamic process of tumor growth was observed, as shown in Figure 5A and B. Our results showed that bo[illegible] tumor volumes and weights were remarkably decreased in the sh-PIM1 group compared with the negative control group (Figure 5C–E). Furthermore, we observed that the PIM1 expression was lower in the sh-PIM1 group in comparison with the negative control group by IHC staining (Figure 5F and G). Much weaker staining of Ki-67 was observed in the Sh-PIM1 group compared with the negative control group (Figure 5F and H). A schematic representation showing PIM1-mediated aggressive behaviors through regulating key molecules of aerobic glycolysis in GBC is shown in Figure 5I. These data indicated that up[illegible]lated PIM1 contributes to the progression of GBC [illegible]rough re[illegible]gramming glucose metabolism via regulating [illegible]y molecules [illegible]f aerobic glycolysis in GBC.

Discussion

To our knowledg[illegible]his is the [illegible]rst stud[illegible]of PIM1 in GBC. We observed that [illegible]M[illegible]was upregu[illegible]d in clinical GBC tissues compared with non-t[illegible]orous gallbladder tissues, and PIM1 expres[illegible]as greater i[illegible]TNM III–IV stages tumors and in tum[illegible]rs with distant metastases present. Clinicopathological [illegible]alysis sugg[illegible]ted that increased PIM1 expression was signi[illegible]ntly cor[illegible]ated with TNM stage, distant metastasis, [illegible]istologic grade, and poor prognosis. Furthermore, our results

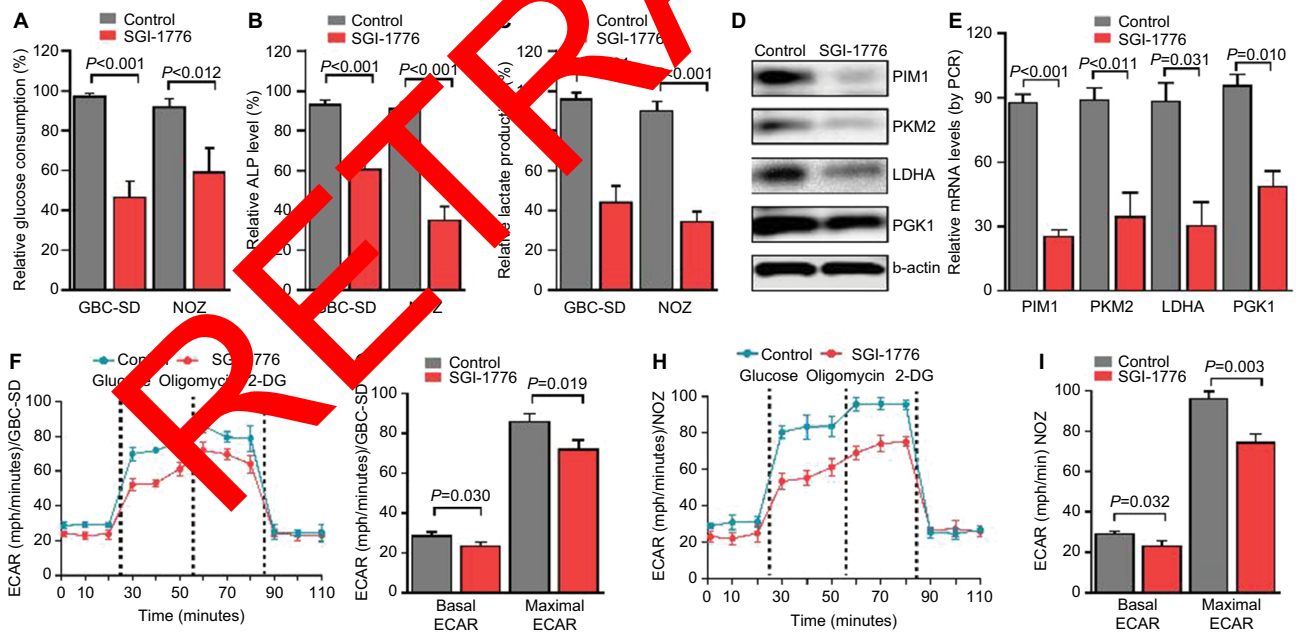

Figure 4 The inhibition of PIM1 regulates glucose metabolism in GBC cells.

Notes: (**A**) Glucose consumption was decreased in GBC-SD and NOZ cells treated with SGI-1776. (**B**) Significantly decreased ATP concentration was found in PIM1-inhibited GBC cells. (**C**) Lactate production in GBC cells was decreased after being treated with SGI-1776. (**D**) Essential glycolytic enzymes involved in the Warburg effect including PKM2, LDHA, and PGK1 expressions were signally decreased in GBC-SD cells treated with SGI-1776 group. (**E**) The mRNA levels of PIM1, PKM2, LDHA, and PGK1 were markedly decreased in PIM1-inhibited GBC-SD cells. (**F–I**) ECARs were measured by the glycolysis stress test in GBC-SD and NOZ cells after the cells were treated with SGI-1776. The basal ECAR and maximal ECAR were significantly decreased in SGI-1776 treated group respectively.

Abbreviations: ATP, adenosine triphosphate; ECARs, extracellular acidification rates; GBC, gallbladder cancer.

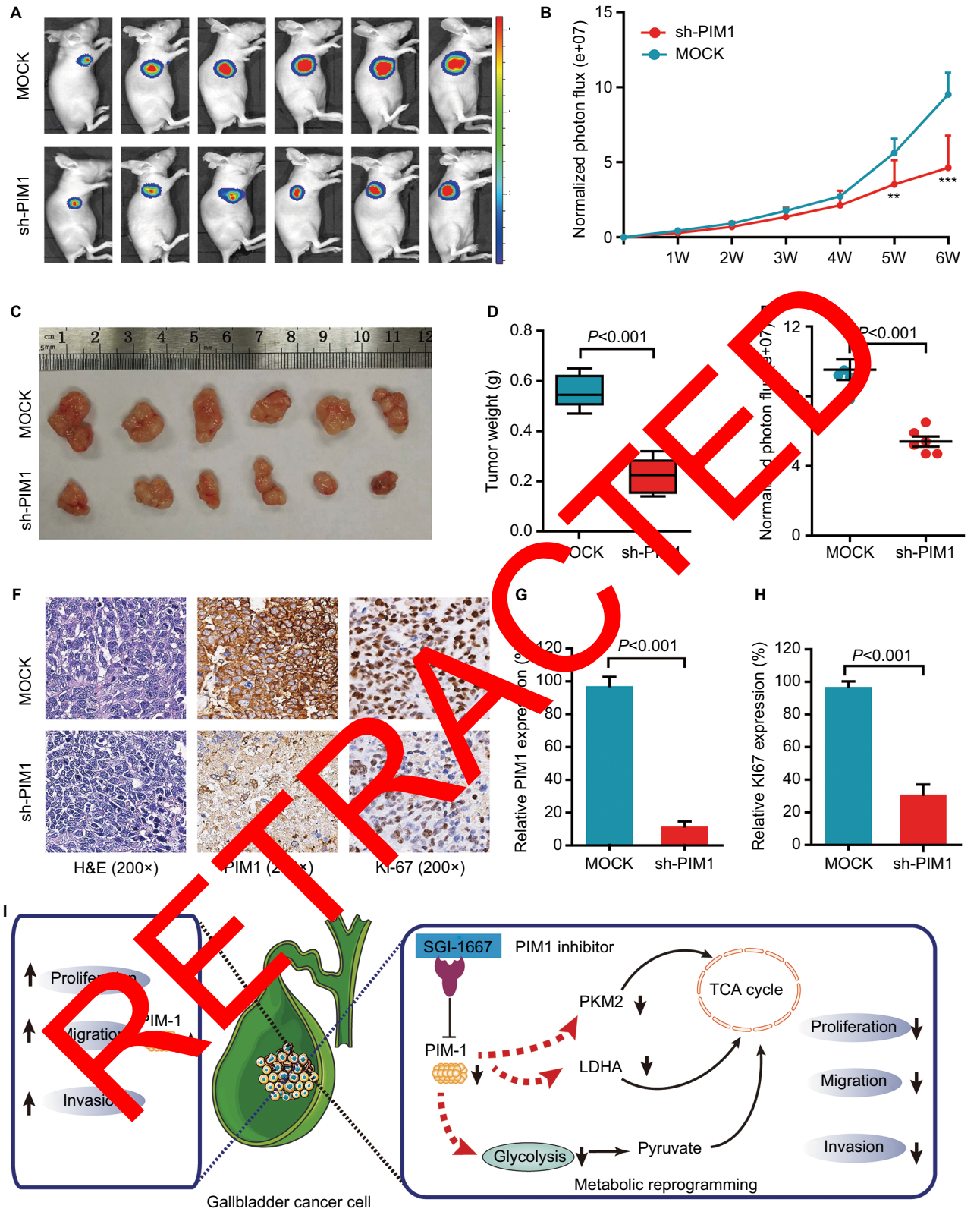

Figure 5 The inhibition of PIM1 suppresses GBC tumorigenesis in vivo.

Notes: (**A**) Images of tumor formation were taken by a live imaging system detecting the luciferase signal. (**B**) The luciferase activity of the sh-PIM1 tumors was lower than that of the MOCK group. Tumor volumes (**C**) and tumor weights (**D**) in sh-PIM1 group were markedly lower than those in MOCK group. (**E**) Tumor luciferase activity in sh-PIM1 group was significantly lower than that of MOCK group. (**F–H**) Sections of xenograft tumors were stained with hematoxylin and eosin, as well as immunohistochemical staining for PIM1. (**I**) Schematic representation showing PIM1-mediated aggressive behaviors through regulating key molecules of aerobic glycolysis in GBC.

Note: **P<0.01, ***P<0.001.

Abbreviations: GBC, gallbladder cancer; TCA, tricarboxylic acid.

indicated that PIM1 expression was an independent prognostic factor of OS in GBC patients (Table 2). Moreover, our survival analysis showed that patients with high expression of PIM1 displayed significantly poorer OS than those who had low PIM1 expression. Consistent with our findings, increased PIM1 has been observed in a variety of tumors and correlated with poor survival, like in glioblastoma multiforme,[8] bladder cancer,[9] hepatocellular carcinoma,[10] colorectal cancer,[20] prostate cancer,[21] and triple-negative breast cancers.[7] All of these results suggested that PIM1 may play a pivotal role in tumor development. As upregulation of PIM1 was involved in tumor progression, this gene could serve as a prognostic biomarker in GBC.

In the present study, functional analyses suggested that downregulation of PIM1 by RNAi or SGI-1776 inhibitor in GBC cells led to a significant suppression of cell proliferation, migration, invasion in vitro, and tumor growth in vivo. In addition, inhibition of PIM1 promoted cell apoptosis and induced cell cycle arrest in vitro. These results suggest this gene plays an oncogenic role. Several studies have shown that PIM1 is an essential oncogene role in many cancers, which was consistent with its functional role in GBC. For example, Brasó-Maristany et al reported that PIM1 could regulate cell death and tumor growth in hepatocellular carcinoma,[10] colorectal cancer,[22] and triple-negative breast cancer.[23] Similar results were observed in clear-cell renal-cell carcinoma[24] and salivary adenoid cystic carcinoma.[25] Based on these results, PIM1 may serve as a promising target for therapeutic intervention.

SMI-4a, AZD1208, and SGI-1776 are inhibitors specific for PIM1, and PIM1 is the first clinically tested inhibitor of the PIM kinase family.[26] Chen et al reported that protein levels of total c-Myc as well as phospho-c-Myc (Ser62), a PIM1 target site, were decreased after SGI-1776 treatment in B-cell chronic lymphocytic leukemia. This finding was suggestive for further study of this inhibitor for treatment of patients with B-cell chronic lymphocytic leukemia.[27] Moreover, inhibition of PIM1 by SGI-1776 could promote the apoptosis of GBC cells, which suggested that PIM1 might be a promising target for advanced GBC. Several studies have revealed that PIM1 inhibitors served as the new drugs for treating triple-negative breast cancers[28] and hematological malignancies[29] in vitro. All these findings further confirmed that aberrantly overexpressed PIM1 may be a cancer-promoting event and PIM1 inhibitor may be a promising drug for anticancer therapy in GBC.

In mechanism explored above, we found that PIM1 played an essential role in the regulation of the glycolysis process. To further clarify the regulation mechanism of PIM1 in glycolysis, we detected the glucose uptake and glycolytic flux in GBC cells. We found that the glucose consumption and key enzymes of glycolysis, such as LDHA[15] and PKM2,[30] were significantly decreased in the PIM1-inhibited group. Furthermore, glycolysis stress and cell mito stress assays suggested that downregulation of PIM1 suppressed glycolysis capacity, and inhibition of PIM1 increased the mitochondrial oxidative phosphorylation ratio, indicating an energy metabolism shift in GBC cells.

For solid tumors, including GBC, cancer cells enable their rapid growth and enormous metabolic needs through the Warburg effect, in which cancer cells enhance the uptake of glucose and aerobic glycolysis.[31] Several studies have shown that upregulation of PIM1 could promote tumor growth, which was similar to our results like colorectal cancer and hepatocellular carcinoma. Wang et al reported that PIM1 expression was markedly overexpressed in response to glucose deprivation-induced metabolic stress through AMP-activated protein kinase signal.[22] Liang et al reported that knockdown of PIM1 could reduce glucose consumption and decrease key enzymes of the glycolytic pathway in hepatocellular carcinoma.[10] Taken together, glycolysis may play an important role in enhancing GBC progression, and PIM1 may promote tumor growth by reprogramming glycolysis. These findings suggest that targeting of PIM1 via inhibitors may be a novel therapeutic intervention for patients with GBC.

Conclusion

Our results revealed that PIM1 was upregulated in clinical gallbladder cancer tissues and positively related with poor outcomes in patients with GBC. Inhibition of PIM1 could significantly suppress GBC cells' proliferation, migration, invasion, and energy metabolism. Moreover, we confirmed the function of PIM1 as a regulator of glycolysis. Based on these findings, the present study provides a better understanding of the function of reprogramming cancer cell metabolism. PIM1 could serve as a biomarker for GBC progression and is a promising target attenuation of cancer cell metabolism reprogramming.

Acknowledgments

This study was supported by funds from the National Natural Science Foundation of China (grant nos. 81702757, 81702346, 81600506, and 81702927); the Medicine Science and Technology Research Project of Henan Province (grant nos. 201602032, 201702001, and 201702032); Youth Innovation Fund of the First Affiliated Hospital of Zhengzhou

University (YNQN2017167, RRS, JL, YNQN2017031, YNQN2017032); Foundation of Henan Educational Committee (18A320038); Tian Qing Liver Disease Research Fund Project of Chinese Foundation for Hepatitis Prevention and Control (TQGB20170012); National Engineering Laboratory for Internet Medical System and Application Open Fund Project (NELIMSA2018P03); The Joint Research Fund of the First Affiliated Hospital of Zhengzhou University and Dalian Institute of Chemical Physics Chinese Academy of Sciences (RRS, JL and ZGR). The funding body had no role in the design of the study, collection, analysis, and interpretation of the data, or in the manuscript writing.

Disclosure

The authors report no conflicts of interest in this work.

References

1. Dwivedi AN, Jain S, Dixit R. Gall bladder carcinoma: Aggressive malignancy with protean loco-regional and distant spread. *World J Clin Cases*. 2015;3(3):231–244.
2. Hundal R, Shaffer EA. Gallbladder cancer: epidemiology and outcome. *Clin Epidemiol*. 2014;6:99–109.
3. Kanthan R, Senger JL, Ahmed S, Kanthan SC. Gallbladder Cancer in the 21st Century. *J Oncol*. 2015;2015:967472.
4. Baig M, Guarino M, Petrelli N. Report on demographics of gall bladder cancer in Delaware and retrospective review of treatment strate[illegible]s for gallbladder cancer in a large community cancer center. *Surg Onco*. 2016;25(2):86–91.
5. Zhu AX, Hezel AF. Development of molecularly targeted ther[illegible]ies in biliary tract cancers: reassessing the challenge[illegible]and [illegible]portuni[illegible]. *Hepatology*. 2011;53(2):695–704.
6. Brault L, Gasser C, Bracher F, Huber K, K[illegible]pp S, Sch[illegible]oller J. PIM serine/threonine kinases in the pathogene[illegible]is and [illegible]era[illegible]of hemato[illegible]gic malignancies and solid cancers. *Haem[illegible]logica*. 20[illegible]95(6):1004–1015.
7. Brasó-Maristany F, Filosto S, Cato[illegible]e S, et al. PIM[illegible]inase regulates cell death, tumor growth and ch[illegible]moth[illegible]y response in [illegible]ple-negative breast cancer. *Nat Med*. 2016;22(11):130[illegible]313.
8. Herzog S, Fink MA, W[illegible]mann K, et al. Pi[illegible]kinase is upregulated in glioblastoma multi[illegible]rme and mediates tumo[illegible]cell survival. *Neuro Oncol*. 2015;17(2[illegible]3–242.
9. Guo S, Mao X, Chen[illegible]t al[illegible]verexpress[illegible]n of Pim-1 in bladder cancer. *J Exp Clin C[illegible]r Res*. [illegible]0;29:161.
10. Leung C[illegible], Wong[illegible]TC, Far[illegible]N, [illegible]al. PIM1 regulates glycolysis and prom[illegible]s tumor p[illegible]gression in[illegible]patocellular carcinoma. *Oncotarget*. 201[illegible]13):108[illegible].
11. Shahruz[illegible]SH, Fakurazi S, Maniam S. Targeting energy metabolism to eliminat[illegible]ncer cells. *Cancer Manag Res*. 2018;10:2325–2335.
12. Sorscher S. M[illegible]d radiographic response of a HER-2-overexpressing biliary cancer to trastuzumab. *Cancer Manag Res*. 2013;9:1–3.
13. Epstein T, Gatenby RA, Brown JS. The Warburg effect as an adaptation of cancer cells to rapid fluctuations in energy demand. *PLoS One*. 2017;12(9):e0185085.
14. Krisher RL, Prather RS. A role for the Warburg effect in preimplantation embryo development: metabolic modification to support rapid cell proliferation. *Mol Reprod Dev*. 2012;79(5):311–320.
15. He Y, Chen X, Yu Y, et al. LDHA is a direct target of miR-30d-5p and contributes to aggressive progression of gallbladder carcinoma. *Mol Carcinog*. 2018;57(6):772–783.
16. Xie H, Tong G, Zhang Y, Liang S, Tang K, Yang Q. PGK1 Drives Hepatocellular Carcinoma Metastasis by Enhancing Metabolic Process. *Int J Mol Sci*. 2017;18(8):1630.
17. Kim YW, Park YK, Yoon TY, Lee SM. Expression of the GLUT1 glucose transporter in gallbladder carcinomas. *Hepatogastroenterology*. 2002;49(46):907–911.
18. Iqbal MA, Siddiqui FA, Gupta V, et al. Insulin enhances metabolic capacities of cancer cells by dual regulation of glycolytic enzyme pyruvate kinase M2. *Mol Cancer*. 2013;12:72.
19. Chen J, Yu Y, Chen X, et al. MiR[illegible]59-5p [illegible]ssociated with poor prognosis and regulates glycolysi[illegible]by repressing [illegible]M2 in gallbladder carcinoma. *Cell Prolif*. 2018:e12[illegible].
20. Liu K, Gao H, Wang Q, e[illegible]t. Hisp[illegible]lin suppres[illegible] cell growth and metastasis by targeting P[illegible]1 through JA[illegible]/STAT[illegible]ignaling in colorectal cancer. *Cancer S[illegible]*2018;109[illegible]):1369–[illegible].
21. Gu H, Liu M, Di[illegible]C, et[illegible]. Hypoxia-responsive miR-124 and miR-144 redu[illegible]hypo[illegible]duced auto[illegible]agy and enhance radiosensitivity of [illegible]ostate cance[illegible]lls via [illegible]ppressing PIM1. *Cancer Med*. 2016;5[illegible]4–1182.
22. Zhang M, Liu [illegible]un H, et al. Pim1 supports human colorectal cancer growth during glu[illegible]se deprivation by enhancing the Warburg effect. *Cancer Sci*. 2018;10[illegible]:1468–1479.
[illegible]. Brasó-Maristany F, Filosto S, Catchpole S, et al. PIM1 kinase regulates cell death, t[illegible]or growth and chemotherapy response in triple-negative breast cance[illegible]*Nat Med*. 2016;22(11):1303–1313.
[illegible]. Zhao B, Li[illegible], Mao J, Zhang Z, Wang Q, Li Q. PIM1 mediates epithelial-[illegible]nal transition by targeting Smads and c-Myc in the nucleus and potentiates clear-cell renal-cell carcinoma oncogenesis. *Cell Death*[illegible]. 2018;9(3):307.
25. Xu J, Zhu X, Li Q, et al. Loss of PIM1 correlates with progression and prognosis of salivary adenoid cystic carcinoma (SACC). *Cancer Cell Int*. 2018;18:22.
26. Mary Photini S, Chaiwangyen W, Weber M, et al. PIM kinases 1, 2 and 3 in intracellular LIF signaling, proliferation and apoptosis in trophoblastic cells. *Exp Cell Res*. 2017;359(1):275–283.
27. Chen LS, Redkar S, Bearss D, Wierda WG, Gandhi V. Pim kinase inhibitor, SGI-1776, induces apoptosis in chronic lymphocytic leukemia cells. *Blood*. 2009;114(19):4150–4157.
28. Horiuchi D, Camarda R, Zhou AY, et al. PIM1 kinase inhibition as a targeted therapy against triple-negative breast tumors with elevated MYC expression. *Nat Med*. 2016;22(11):1321–1329.
29. Garcia PD, Langowski JL, Wang Y, et al. Pan-PIM kinase inhibition provides a novel therapy for treating hematologic cancers. *Clin Cancer Res*. 2014;20(7):1834–1845.
30. Wang C, Jiang J, Ji J, et al. PKM2 promotes cell migration and inhibits autophagy by mediating PI3K/AKT activation and contributes to the malignant development of gastric cancer. *Sci Rep*. 2017;7(1):2886.
31. Guo W, Qiu Z, Wang Z, et al. MiR-199a-5p is negatively associated with malignancies and regulates glycolysis and lactate production by targeting hexokinase 2 in liver cancer. *Hepatology*. 2015;62(4):1132–1144.

Supplementary materials

Table S1 Cell lines used in this study

Cell lines	Cell type	Source	Country
GBC-SD	Gallbladder carcinoma cell	Cell Bank of the Chinese Academy of Science	Shanghai, China
NOZ	Gallbladder carcinoma cell	Cell Bank of the Chinese Academy of Science	Shanghai, China
SGC-996	Gallbladder carcinoma cell	Cell Bank of the Chinese Academy of Science	Shanghai, China
OCUG-1	Gallbladder carcinoma cell	Cell Bank of the Chinese Academy of Science	Shanghai, China

Table S2 Information on antibodies used in this study

Antibody	WB	IHC	IF	Specificity	Company
β-Actin	1:5,000	/	1:200	Mouse monoclonal	Proteintech Group, Wuhan, China
PIM1	1:5,000	1:100	1:250	Rabbit monoclonal	Abcam, Cambridge, MA, USA
Ki-67	/	1:500	/	Rabbit polyclonal	Proteintech Group, Wuhan, China
Alexa (Fluro594)	/	/	1:200	Goat anti-Rabbit	Jackson Immunoresearch, West Grove, PA, USA
Alexa (Fluro488)	/	/	1:200	Goat anti-Mouse	Jackson Immuno Research, West Grove, PA, USA

Abbreviations: WB, Western blotting; IF, immunofluorescence.

Table S3 siRNA sequence used in this study

siRNA	Sense sequence	Anti-sense sequence
PIM1	5′-GAUAUGGUGUGUGGAGAUAtt-3′	5′-UAUCUCCACACACCAUAUCtt-3′
NC	5′-UUCUCCGAACGUGUCACGUTT-3′	5′-ACGUGACACGUUCGGAGAATT-3′

Table S4 qRT-PCR primer sequence used in this study

Name	Forward primer sequence	Reverse primer sequence
PIM1	5′-CGGCAAGTTGTCCTAGAC	5”- CCTGGAGGTTGGGATGCTCT-3′
PKM2	5′-ATTATTTGAGGAACTCCCGCCT-3′	5′-ATTCCGGGTCACAGCAATGATGG-3′
LDHA	5′-ATGGCACTAAAGGACA-3′	5′-GCAACTTGCAGTTCGGGC-3′
PGK1	5′-ATGCAAGAGGCCAAGCAC-3′	5′-AGCCACAGCCTCAGCATATTTC-3′
β-actin	5′-CTCCATCCTGGCTCGCTGT-3′	5′-GCTGTCACCTTCACCGTTCC-3′

Abbreviation: qRT-PCR, quantitative real-time PCR.